

Effect Evaluation of the Interaction Between the Atmosphere and the Soil on the Ngamakosso's Embankment Stability, Talangai, Brazzaville, Republic of Congo

Obami-Ondon Harmel^{1,*}, Kempena Adolphe², Ngoma Mpemba Charmella Franche Amina²,
Rafael Guardado Lacaba³, Antonio Olimpio Gonçalves⁴, Tathy Christian¹

¹Mechanical, Energy and Engineering Laboratory, Higher National Polytechnic School, Marien Ngouabi University, Brazzaville, Republic of Congo

²Department of Geology, Faculty of Sciences and Techniques, Marien Ngouabi University, Brazzaville, Republic of Congo

³Department of Geology, Faculty of Mines and Geology, Higher Institute of Mines and Metallurgy, Moa, Cuba

⁴Departement of Geology, Faculty of Sciences, Agostinho Neto University, Luanda-Angola

*Corresponding author: harmelobami@gmail.com

Received July 11, 2024; Revised August 12, 2024; Accepted August 19, 2024

Abstract The stability of an embankment is analyzed by determining its safety factor. The present work consists of analyzing the effect of atmosphere-soil interaction on the stability of the embankment located in the Ngamakosso district (Talangai, Brazzaville, Congo Republic). The aim of this work is to carry out an in-depth study of this embankment using the finite element method in order to evaluate its stability. The study of the stability of natural slope using finite element method gave a low safety factor showing that the slope is unstable. However, earthworks by softening the slope angle as well as the establishment of vetiver-type plant cover had appositive influence and constituted an effective means of stabilizing this slope. The results obtained after these analyzes indicate that the embankment is in a satisfactory state of stability.

Keywords: Ngamakosso, embankment, modeling, atmosphere, soil

Cite This Article: Obami-Ondon Harmel, Kempena Adolphe, Ngoma Mpemba Charmella Franche Amina, Rafael Guardado Lacaba, Antonio Olimpio Gonçalves, and Tathy Christian, "Effect Evaluation of the Interaction Between the Atmosphere and the Soil on the Ngamakosso'S Embankment Stability, Talangai, Brazzaville, Republic of Congo." *American Journal of Environmental Protection*, vol. 12, no. 3 (2024): 31-41. doi: 10.12691/env-12-3-1.

1. Introduction

Landslides as natural phenomenon is part of a set of movements along the slopes. They are common and constitute a permanent risk in almost all regions of the world with a significant number of victims among local populations and on construction works [1,2]. Some landslides can be considered as a natural evolutionary process of the site. However, it should be noted that certain landslides can be triggered by certain human actions on the environment disrupting the natural balance of a site, giving to a process of disruption of already stable slopes [3,4,5]. In Congo, several risks have been cataloged, including landslides which represent a threat to most of its large cities. In such circumstances, it must be recognized that the geomorphology of the northern districts of Brazzaville essentially contains steep slopes, frequently affected by spectacular land movements. These natural phenomena constitute one of the most common risks in the northern part of this city, mainly in neighborhoods

such as Talangai, Mikalou, Nkombo, Massengo [6]. Therefore, Brazzaville City, through its geomorphological context, appears to be vulnerable to landslides. Landslides represent a serious problem in almost all northern districts of Brazzaville, because they cause economic or social losses on private and public properties [7]. The present work aims to evaluate the influence of the interaction between atmosphere and soil on the Ngamakosso's embankment.

2. Study Area

The study area is located in the Talangai district of the city of Brazzaville, in the Republic of Congo with the following geographic coordinates: 015° 18'35"E; 04°11'88"S (Figure 1).

The study area has a tropical climate with a dry season from June to September and a rainy season from October to May. total Precipitations are 1345 millimeters per year and the average temperature of the coldest month (July) is 23.6°C and that of the hottest month (April) is 27.7°C.

High humidity ranging from 70 to 80% is recorded. With the phenomena of climate change, temperatures in the city of Brazzaville have seen a marked increase. Thus, during the rainy season, it rains heavily and it is observed intense heat throughout the day [8,9]. The vegetation is marked by forests and savannahs with a contrasting landscape juxtaposing the reliefs of the plateaus and plains [10]. Brazzaville has diverse types of soils, depending on the bedrock we distinguish soils formed on the polymorphic sands with clay content and very low mineral reserves, soils formed on the Inkisi sandstone with a sandy-clayey texture and soils formed on heterogeneous alluvium of the Congo River and its tributaries. In general, these sandy soils -clayey are poor in organic matter [11,12]. The geological formations met in the region according to [13,14] are divided into three large groups with sedimentary deposits described from bottom to top as follows: the Inkisi Group, the Stanley-Pool Group and the Téké Plateaux Group. The Inkisi Group with a height ranging from 600 to 700 m, crops out in the southwest of Brazzaville. This geological group of fluvial origin rests in angular unconformity on the Mpioka Group and is subdivided into three levels [15]. The Stanley-Pool Group dated from the Upper Jurassic-Lower Cretaceous is made up of clayey and marly sandstones and rests in ravinement unconformity on the sandstones of the Inkisi group [13]. However, the Téké Plateaux Group is made up of locally silicified aeolian sands with two levels (Ba1 and Ba2) which correspond to polymorphic sandstones of Paleogene age and ocher-yellow sands of Neogene age, respectively.

The ocher yellow sands are separated from level Ba1 by a stone line of fluvial, alluvial or colluvial origin [16,17].

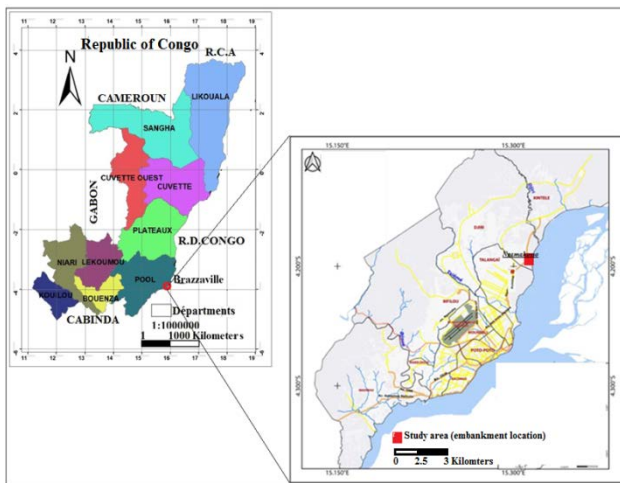


Figure 1. Study area location

3. Materials and Methods

The field approach then made it possible to inspect the study area and carry out on-site measurements concerning the length, height and dip of the Ngamakosso's embankment. These measurements allowed us to define the geometry of the embankment. The laboratory study consisted of processing data collected in the field and those related to the physical and mechanical properties of soils [6]. This makes it possible to analyze the technical parameters of the embankment to carry out calculations

using the finite element method in plaxis 2D, in order to quantitatively evaluate the effects of embankment instability parameters such as geometry, hydraulic conditions and soil mechanical characteristics.

Calculation of the safety factor (Msf, SMsf)

The reduction of mechanical characteristics (Phi-c reduction) is an option available in PLAXIS 2D which allows the calculation of safety factors. In the Phi-c reduction approach, the characteristics of "φ and c" of the soil are gradually reduced until the embankment rupture. The characteristics of the interfaces, if any, are reduced at the same time. The total safety factor (SMsf) allows defining the value of soil characteristics at a given stage of the analysis as follows:

$$\sum Msf = \frac{\tan \phi \text{ input}}{\tan \phi \text{ reduced}} = \frac{C \text{ input}}{C \text{ reduced}} \quad (1)$$

Hence, the characteristics denoted 'input' refer to the material properties and the characteristics denoted 'reduced' refer to the reduced values used during the analysis. Unlike other coefficients, Msf is set to 1.0 at the start of a calculation to use unreduced values of material characteristics. Thus, a calculation of Phi-c reduction was carried out using the forward loading procedure. The incremental multiplier Msf was used to specify an increment of the resistance reduction factor for the first calculation step. This increment is set to 0.1 by default, which is generally a good starting value. The strength parameters were thus reduced step by step automatically until all additional steps had been taken. By default, the number of additional steps was set to 30 for this type of calculation, but a larger value (up to 1000) could be given, if necessary. However, it was still necessary to check whether the last calculation step led to a generalized failure mechanism. If this was the case, the factor of safety (FOS) was calculated as follows:

$$FOS = \frac{\text{Available strength}}{\text{shear strength}} = \text{Valor of Msf} \quad (2)$$

When the failure mechanism has not fully developed, the calculation should be repeated with an increased number of additional steps. Using the Phi-c reduction option in combination with advanced soil models, these models will actually behave according to the Mohr-Coulomb model, since the dependence of stiffness with the stress state and the effects of work hardening were excluded. The module calculated at the end of the previous calculation step for the stress state obtained was used as a constant stiffness during the calculation of Phi-c reduction.

Slope model

The studied embankment is located in an area representing a hill with a steep slope (Figure 2). The soils met in the study area consist of loamy sands with a low clay content [6]. Table 1 presents the characteristics of the geometry of the slope model studied.

In this step we represented the slope model in PLAXIS (input) by defining the data, the choice of the "MOHR-COULOMB" soil behavior law. We fixed the ends of the slope to prevent horizontal and vertical displacements in the horizontal end, as well as vertical displacements in the

vertical ends, so that the design boundaries do not influence the results. This section allowed the creation of a mesh of the model with a triangular element of 15 nodes, and then we generated the pore pressures of the slope in PLAXIS 2D. The simulations were carried out on the selected model, getting as close as possible to reality in several stages. The first step concerned the meshing of the model followed by the choice of a number of zones for which the notion of refining was applied to the treated locations. The second step concerned the assignment of behavioral laws. For our case; an elastoplasticity law was granted to all the zones representing the numerical model. The Mohr-Coulomb criterion used includes the following factors: soil density, intrinsic soil properties such as cohesion, internal friction angle, expansion angle, Young's modulus and Poisson's ratio which are essential for elastic calculation. The third step considered fixing the boundaries of the model, according to the vision of the calculator and the case treated, to give a certain logic to its behavior. Before starting the limit state resolution, it was essential to initialize the constraints in the model by calculating the stresses at rest using the Jacky formula as follows:

$$KB = 1 - \sin\phi'(3); \text{ hence, } \sigma_h = K_0 \cdot \sigma_v \quad (3)$$

We used the effect of gravity (g), in order to accelerate the calculation when starting with the initial conditions. In order to obtain the factor of safety (FOS), the numerical code used the strength factor reduction method (c-φ). The model used in the parametric study takes into consideration the calculation of the factor of safety (FOS). The numerical analyzes carried out by the PLAXIS 2D

code determined the value of the factor of safety by the technique of reducing the intrinsic parameters of the soil (cohesion and the angle of internal friction). The geotechnical properties of the materials used in the modeling are illustrated in Table 2 and Table 3.

Table 1. Characteristics of the slope geometry

Nature of layers	Height (m)		Width (m)	Slope (°)	
	Hmax	Hmin			
Silty sand with organic matter	3.5	20	8	20	69
Silty sand with little clay content	16.5				

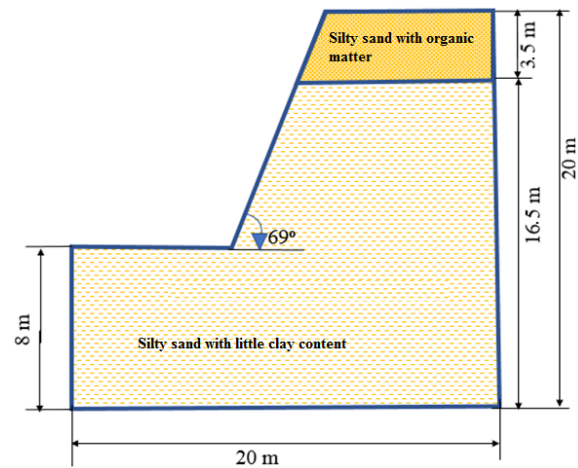


Figure 2. Slope model geometry

Table 2. Geotechnical parameters of the layers forming the profile of the slope studied before human intervention

Nature	γ_{unsat} (KN/m ³)	γ_{sat} (KN/m ³)	Cref (KPa)	Φ (°)	Ψ (°)	Eref (KPa)	V	K(m/s)
Silty sand	18	19.7	4.3	40.1	0	2.104	0.3	0
Yellow Sand	18.8	20	10.7	40.2	3	3.104	0.3	0.432

Table 3. Geotechnical parameters of the layers forming the profile of the slope studied after human intervention

Nature	γ_{unsat} (KN/m ³)	γ_{sat} (KN/m ³)	Cref (KPa)	Φ (°)	Ψ (°)	Eref (KPa)	V	K(m/s)
Loamy sand	18	19.7	2	29	0	2.104	0.3	0
Yellow Sand	18.8	20	2.3	30	3	3.104	0, 3	0.432

Table 4. Geotechnical parameters of the soil

Nature	γ_{unsat} (KN/m ³)	γ_{sat} (KN/m ³)	Cref (KPa)	Φ (°)	Ψ (°)	Eref (KPa)	V	K(m/d)
Loamy sand	18	19.7	4.3	40.1	0	2.104	0.3	0.216
Yellow Sand	18.8	20	10.7	40.2	3	3.104	0.3	37324.8

Parametric study

In this section, it is studied the influence of the inclination of the embankment as a function of the angle of the slope, the values of which vary between 60.10° and 46.2° while keeping the other parameters fixed. We also examined the influence of the water table by varying its water level. The values of which vary between 4 m and 20 m depth relative to the head of the embankment and by keeping the other parameters fixed. Then, we studied the effect of vegetation by inserting 3 m depth of the roots of vetiver plant along the slope and while keeping the other parameters fixed.

Study of infiltrations effect

Here, we examined the effect of infiltrations by using monthly rainfall data from Brazzaville (ANAC, 2023). To do this, according to the requirements of the software, we used the time in days. So, the permeability values, which are initially expressed in m/s, will be expressed in m/day using the following formula: 1 m/s = 86400 m/d. From where, the permeability of the yellow sands K= 0.432m/s becomes K= 37324.8 m/d (Table 4) and the permeability of silty sands K= 0m/s, given that the software cannot calculate the infiltration phase with a zero value, and according to the USCS standard, the K values for silty

sands vary between 10-8 and 5.10-6 m/s. for this purpose, we considered $K= 0.0000025$ or $2.5.10-6$ m/s; that is to say the value $K= 0.216$ m/d after conversion (Table 4).

The rainfall data being in millimeters per month (mm/month), they were converted into meters per month (m/month). Then, into meters per day (m/d) before entering them into the software (Table 5).

Table 5. Monthly rainfall in Brazzaville 2023

Years	Month	Monthly rainfall in mm/month	Monthly rainfall in m/month	Monthly rainfall in m/day
2023	January	412.7	0.4127	0.013
2023	February	318.6	0.3186	0.010
2023	March	190.3	0.1903	0.006
2023	April	262.6	0.2626	0.008
2023	May	157	0.157	0.005
2023	June	0.5	0.0005	0.00001
2023	July	0	0	0
2023	August	0	0	0
2023	September	16.3	0.0163	0.0005
2023	October	115.8	0.1158	0.004
2023	November	176.1	0.1761	0.006
2023	December	279.9	0.2799	0.009

Then, these rainfalls were divided into three periods and for each period we calculated the average from the sum of monthly rainfall, then divide by the number of

months. The first period is from January to May. However, the second period from June to August and the third period from September to December. After calculation, the values obtained were 0.0084, 0 and 0.0048 for periods 1, 2 and 3 respectively. Therefore, it is from these rain intensity values that we evaluated the influence of infiltration on the stability of the embankment for periods 1, 2 and 3.

4. Results

The results of this work are based on the analysis of embankments in various conditions with two different types of soils. They also take into account the effects of stormwater infiltration and precipitation intensity, as well as slope geometry.

Figure 3 shows vertical and horizontal displacements with their corresponding values of factor of safety.

Displacements

The analysis of the natural slope gave a low safety factor of around 0.7957 (Figure 3b), indicating an unstable slope. An effective stress of -322.66 kN/m² (Figure 3c), a total displacement of 0.445 m (Figure 3a), a vertical displacement of 0.336 m (Figure 3b) and a horizontal displacement of 0.334m (Figure 3c).

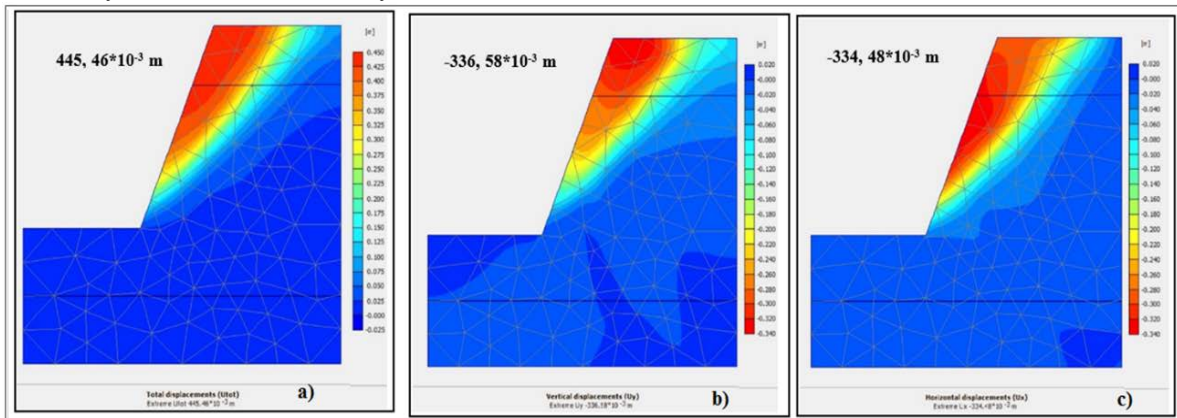


Figure 3. a) Total displacement as well as its value; b) Vertical displacement as well as its value; c) Horizontal displacement as well as its value

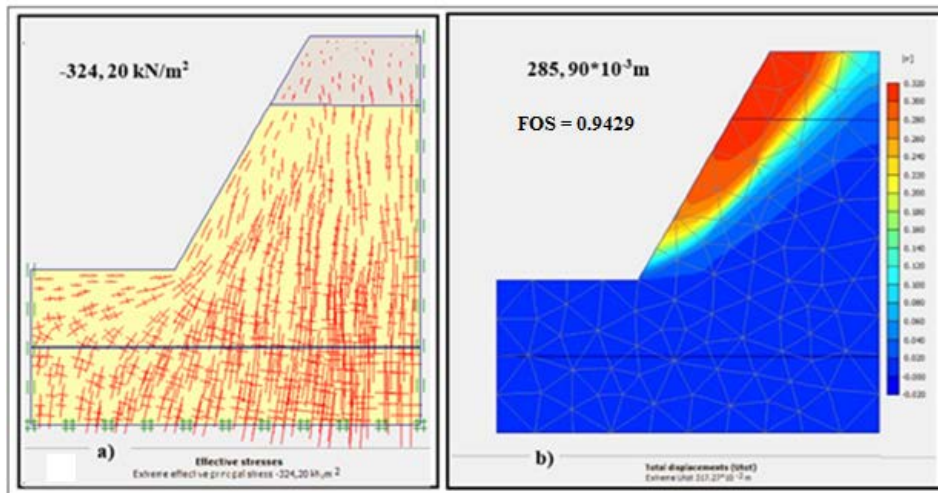


Figure 4. Case of slope 1.5H:1V: a) Effective constraint with its value; b) Total displacement with its value with the value of the safety factor

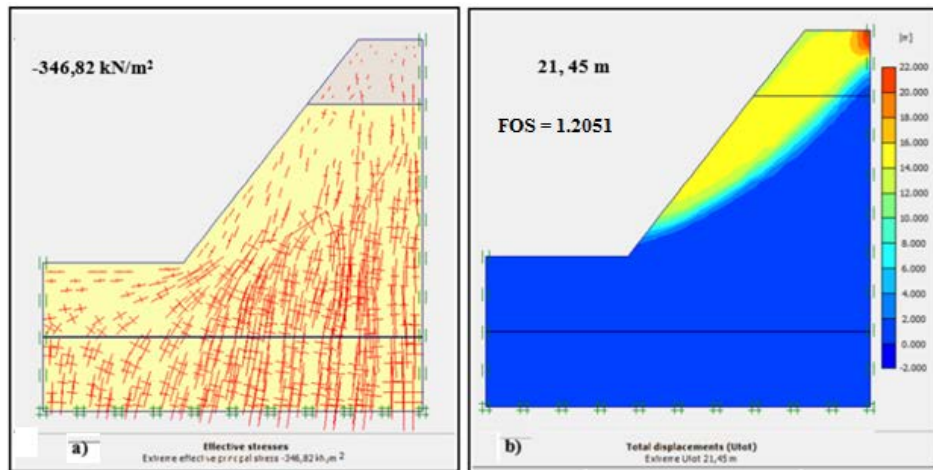


Figure 5. Case of the slope at 2H: 1V: a) effective stress as well as its value; b) Total displacement with the value of the safety factor of the earthed slope 2 as well

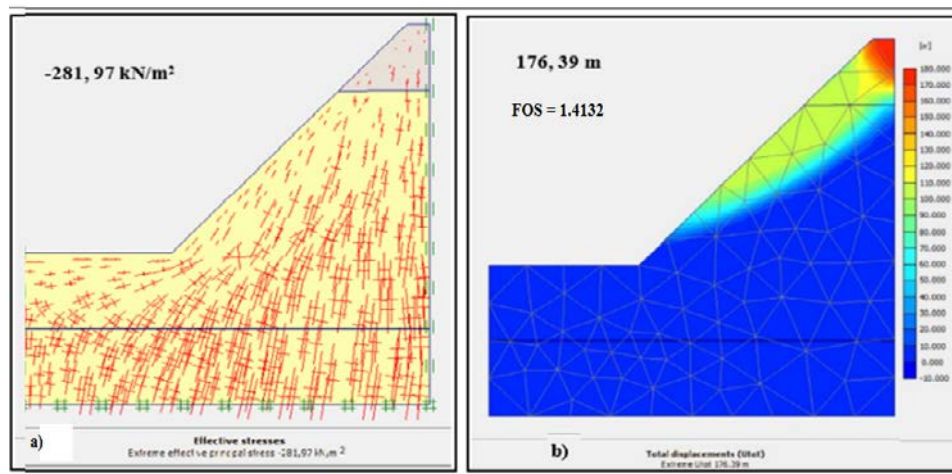


Figure 6. Case of the slope at 2.5H: 1V: a) effective stress as well as its value; b) Total displacement with the value of the safety factor of the earthed slope 3

Effects of slope inclination on the embankment stability

This analysis was carried out by evaluating the influence of the slope inclination when decreasing the slope angle. To achieve this, we used the 1.5H:1V earthworks simulations; 2H:1V and 2.5H:1V, to know at what slope the embankment is stable. The initial slope is represented by 1H:1V which corresponds to the slope angle of 69° . Figure 4 illustrates the case of the slope 1.5H:1V, of which case a) represents the effective stress with its corresponding value and case b) takes into account the total displacement with its corresponding value and the value of the safety factor as well. The analysis of the stability of the slope at 1.5H:1V gave a safety factor of around 0.9429 (Figure 4b), the slope is unstable, an effective stress of -324.20 kN/m^2 (Figure 4a) and a total displacement $285.90 \cdot 10^{-3} \text{ m}$ (Figure 4b), the color scale of which clearly shows this instability of the slope, while noting that the dark orange color in the figure corresponds to the total displacement value.

Figure 5 shows the case of the slope at 2H:1V, from where the value of the safety factor of the earthen slope 2 is observed (Figure 5a), the effective stress with its corresponding value (Figure 5b) and the total displacement with its corresponding value (Figure 5c) . A

total displacement of 21.45m (Figure 5c) is observed, illustrating the stability of the slope thanks to the color scale, from which we see that the orange color observed along the slope in the previous case has disappeared and was replaced by the color yellow. Figure 2 a) shows the case of the slope at 2H: 1V with the value of the safety factor of the earthed slope, an effective stress as well as its value (Figure 2 b) and a total displacement as well as its value (Figure 2c). The results obtained show a safety factor of the order of 1.2051 (Figure 5a) with notable stability, an effective stress of -346.82 kN/m^2 (Figure 5b) and a total displacement of 21.45m (Figure 5c), showing the stability of the slope thanks to the color scale, of which the orange color previously observed along the slope has disappeared and been replaced by the yellow color.

Figure 6 illustrates the case of the slope at 2.5H: 1V the effective stress with its value (Figure 6a) and the displacement with the value of the safety factor of the earthed slope 3 (Figure 6b).

During this analysis of Figure 7, we noted that the factor of safety (FOS) increased respectively from 0.9429 to 1.2051 up to 1.4132 as we decreased the slope of the embankment by 1, 5H:1V, 2H:1V and 2.5H:1V respectively. For the first case we note an instability, for the second case questionable stability is observed and for

the last case we noted satisfactory stability of the embankment.

The values of the factors of safety obtained during this analysis are represented in Table 6.

It is important to consider that the angle of 1H:1V represented in Table 6 corresponds to the natural slope before human intervention.

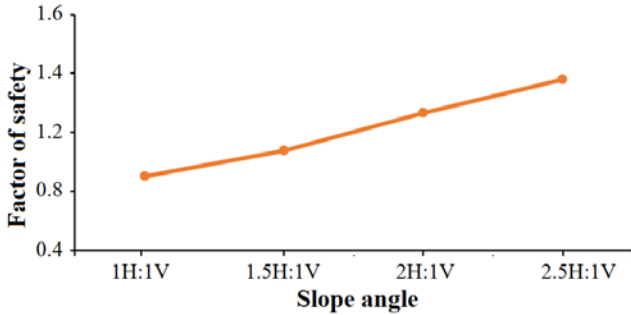


Figure 7. Curve of the factor of safety as a function of the slope angle

Table 6. Factors of safety with types of slopes

Types of slopes	Corresponding angle in degree (°)	Factor of safety
1H:1V	69	0.7957
1.5H:1V	60.10	0.9429
2H:1V	52.52	1.2051
2.5H:1V	46.2	1.4132

Influence of the variation of the horizontal water table on the stability of the slope

The analysis of the stability of unsaturated soil slopes considering suction is discussed. Thus, the influence of the variation in the depths of the horizontal water table is evaluated. For this, the level of the water table was assumed to be at a certain depth (l) and the initial level of the water table is located 4 m from the foot of the embankment (Figure 8). To evaluate the influence of the different depths of the water table on the slope, the analyzes were carried out using l/H ratios between 0 and 1

at an interval of 0.2. It is however important to remember that the analysis began at the level of the head of the embankment which corresponds to the ratio l/H=0 and we stopped at the ratio l/H=1 which corresponds to the initial level of the tablecloth. During this evaluation, we used two cases of embankment: the initial embankment at 1H:1V and the embankment leveled at 2.5H:1V by applying the same procedure previously described.

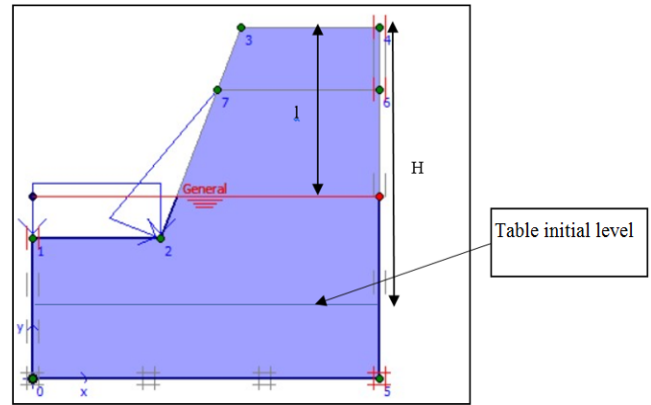


Figure 8. Model boundary conditions

Table 7 as well as Figures 9 and 10 show the values of the factors of safety obtained after evaluation of the different depths of the horizontal water table for the two cases used.

Table 7. Summary table of values of factors of safety depending on the l/H ratio

	1H:1V	2.5H:1V
Depth of the table	Factor of Safety (FOS)	
w/H = 0	1.2841	1.8674
l/H = 0.2	0.9043	1.5092
l/H = 0.4	0.7989	1.3873
l/H = 0.6	0.7832	1.3368
l/H = 0.8	0.7716	1.3788
l/H = 1	0.7653	1.3773

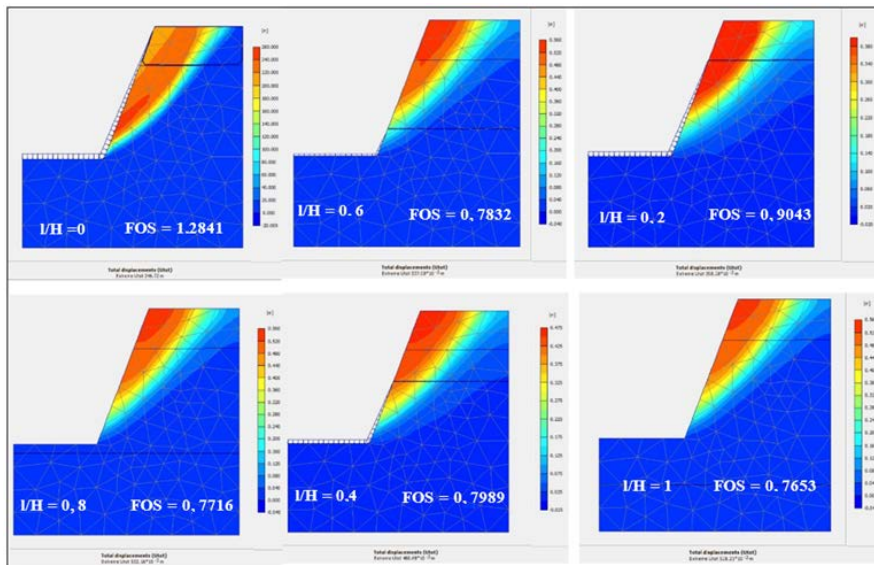


Figure 9. Failure mechanisms with different depths of the horizontal water table in the case of the slope at 1H:1V

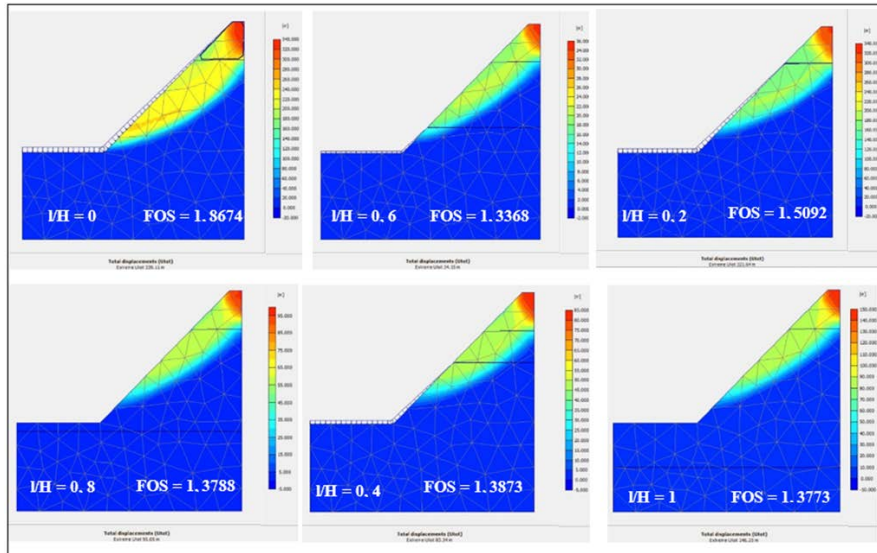


Figure 10. Rupture mechanisms of the different depths of the horizontal water table in the case of the slope at 2.5H:1V.

In the case of 1H:1V, when the embankment is completely submerged ($l/H = 0$), the factor of safety is 1.2841. The latter decreased as the l/H ratio increases, that is to say as the water table level decreases. The critical level of the water table which gives the minimum factor of safety is at $l/H = 1$ with a value of $FS = 0.7653$ (Table 7 and Figure 9).

In the case of 2.5H:1V, when the embankment is completely submerged ($l/H = 0$), the factor of safety factor is 1.8674. Here, the critical level of the water table which gives the minimum safety factor is at $l/H = 0.6$ with a value of $FS = 1.3368$ (see Table 7 and Figure 9). We point out that we also calculated the safety factor without a layer in both cases and the values obtained are as follows: 0.8011 and 1.3786 respectively for the slopes of 1H:1V and 2.5H:1V. During this analysis we noted that when we increase the depth of the horizontal water table, the safety factor also increases; except in the case of the slope at 2.5H:1V where the safety factor decreased to the level $l/H = 0.6$ ($FOS = 1.3368$), then started to increase again from $l/H = 0.4$. Figure 11 shows the evolution of the safety factor curve as a function of the l/H ratio in the two slope cases.

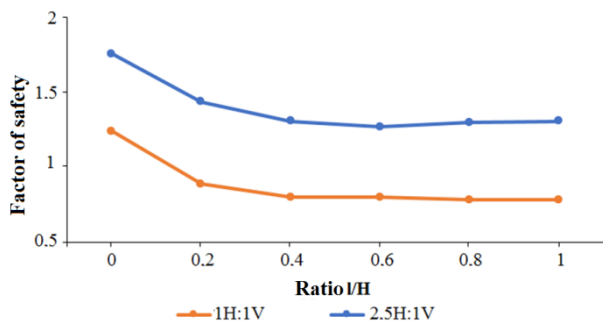


Figure 11. Curves of the safety factor as a function of the l/H ratio for the two slope cases

Influence of vegetation

In this section, the influence of vegetation on slope stability is taken into account. Slope stability was assessed using “vetiver” plant roots along the slope, where these increased soil cohesion by more than 10 kPa at this

distance. So, the cohesion of the yellow sand which was 10.7 kPa has become 20.7 kPa and the cohesion of the silty sand which was 4.3 kPa is now 14.3 kPa. For this, we considered 3 m of vetiver plant roots for the simulations in all cases (1H:1V; 1.5H:1V; 2H:1V; 2.5H:1V). Figure 12 a) shows the safety factor for the slope at (1H:1V), an effective stress and its value are observed in Figure 12 12), as well as the total displacement with its corresponding value in Figure 12 c).

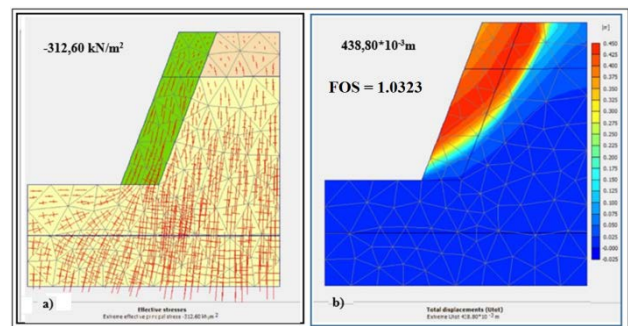


Figure 12. 1H:1V: a) effective stress as well as its value; b) Total displacement with the factor of safety

The results obtained during this analysis show a safety factor of the order of 1.023 (Figure 12 b), referring to a state of stability, an effective stress of -312.60 kN/m² (Figure 12 a) and a displacement total with a value of 0.438m (Figure 12 b), on the embankment, from where we notice the presence of a light orange color.

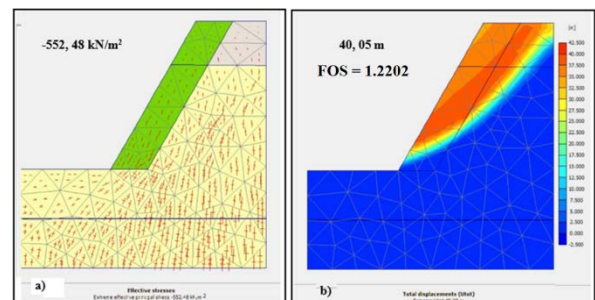


Figure 12. Slope 1.5H:1V: a) effective stress with its value; b) Total displacement with the value of the factor of safety

Figure 13 b shows the value of the safety factor in the case of the slope at 2H:1V, an effective stress and its value are observed in Figure 13 b) and a total displacement with its value in Figure 13 c). The analysis of the stability of the slope at 2H: 1V with the roots of vetiver plants gave a safety factor of around 1.3737 (Figure 13b), which demonstrates that the slope is stable. An effective stress of -535.37 kN/m² is observed in Figure 13a and a total displacement of 41.73 m in Figure 13b), whose green and yellow colors observed along the slope confirm the stability of said slope.

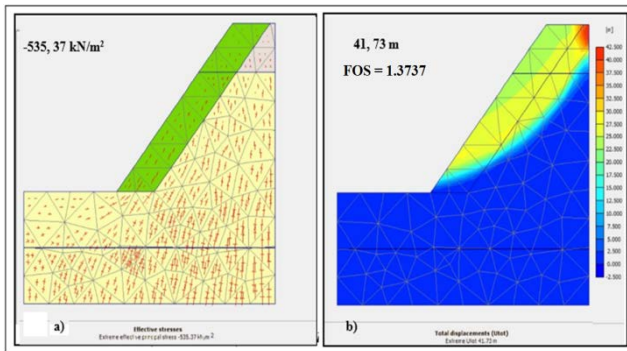


Figure 13. Slope at (2H:1V; a) effective stress as well as its value; b) Total displacement with the value of the safety factor

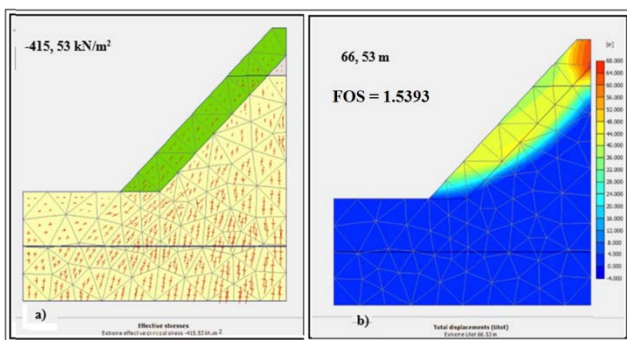


Figure 14. slope at 2.5H:1V: a) effective stress as well as its value; b) Total displacement with a) value of the safety factor

Figure 14a) shows the value of the safety factor in the case of the slope at (2.5H:1V), the effective stress and its value are presented in Figure 14 a) and the total displacement with its corresponding value in Figure 14 vs). The analysis of the stability of the slope at 2.5H:1V with the vetiver plant roots gave a safety factor of the order of 1.5393 (Figure 14b), the slope shows guaranteed stability; an effective stress of -415.53 kN/m² (Figure 14b) and a total displacement of 66.53 m (Figure 14b), the displacement scale clearly shows stability of the slope. The analysis of the influence of vegetation on the stability of the slope shows that the roots of vetiver plants increase the values of the safety factors of all slopes (Figure 15). For the 1H:1V slope, without vetiver the safety factor is 0.7957 and with vetiver the latter is 1.0323. For the 1.5H:1V slope, without vetiver the safety factor (FOS) is 0.9429 and with vetiver it is 1.2202. For the 2H:1V slope, without vetiver the factor (FOS) is 1.2051 and with vetiver it is 1.3737 and

for the 2.5H:1V slope, without vetiver the safety factor is 1, 4132 and with vetiver it is 1.5393.

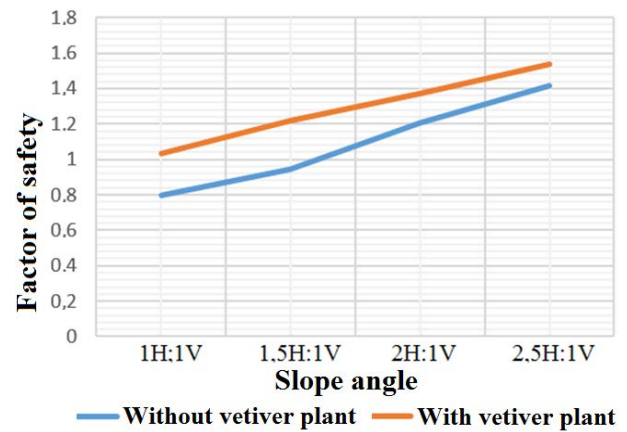


Figure 15. curves of safety factors as a function of the angle of the slope (without vetiver and with vetiver)

The values of all the safety factors obtained after analysis of the slopes without vetiver and with vetiver are represented in [Table 8](#).

Table 8. Summary table of the different types of embankment without vetiver and with vetiver with the values of their respective safety factors

Type of slope	Factor of Safety (FOS)	
	Without vetiver	With vetiver
1H:1V	0.7957	1.0323
1.5H:1V	0.9429	1.2202
2H:1V	1.2051	1.3737
2.5H:1V	1.4132	1.5393

Influence of infiltrations

The influence of infiltration is analyzed without taking into account soil suction. To do this, we assessed the stability of the slope using monthly rainfall data from Brazzaville 2024. The following results were obtained after analysis by simulation of infiltration based on rainfall intensities for each period. We note that the slope is considered to be impermeable at its base and the slopes analyzed are the slopes at 1H:1V and 2.5H:1V. For the case of the 1H:1V slope, period 1 characterized by a rain intensity of 0.0084 m/day gave the results before the rain and after the rain. The results before the rain are presented in period 2. Figure 15 representing the case of the 1H:1V embankment shows Project mesh with Plaxis 2D in Figure 15 a), the initial conditions and the value of the safety factor of the period 1 (Figure 15 b) and the total displacement for period 1 in Figure 15 c). The analysis of the stability of the slope at 1H:1V during the first period which goes from January to May gave a safety factor of around 0.7625 (Figure 15b), a total displacement of 1.398m (Figure 15c). In Figure 16 we observe period 2 is characterized by a rain intensity of 0 m/d. There was no rain during this period so we considered the results before the rain and period 3 characterized by a rain intensity of 0.0048 m/d gave the following results:

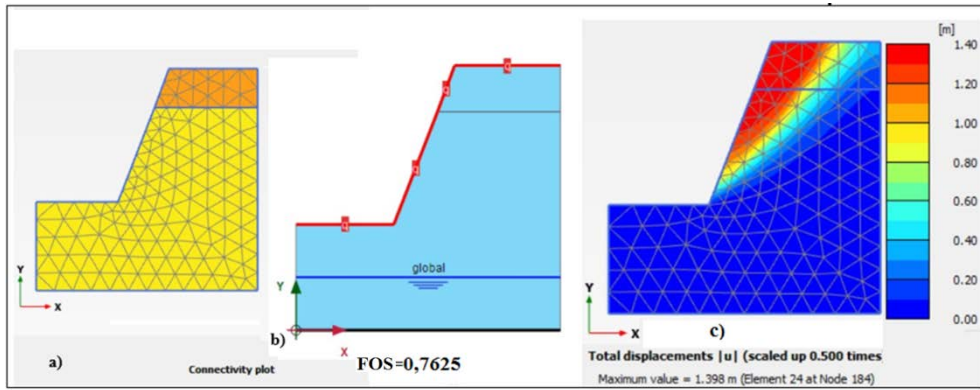


Figure 15. Case of slope 1H:1V: a) Project mesh with Plaxis 2D Connect version; b) initial conditions and the value of the FOS of period 1; c) Total travel for period 1

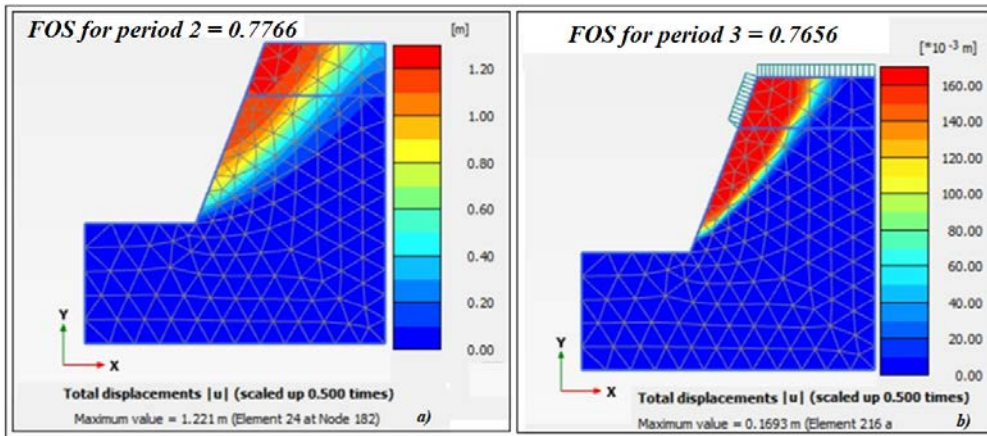


Figure 16. Case of the slope at 1H:1V: a) Total displacement for period 2 as well as the FOS value; b) Total displacement for period 3 as well as the FOS value

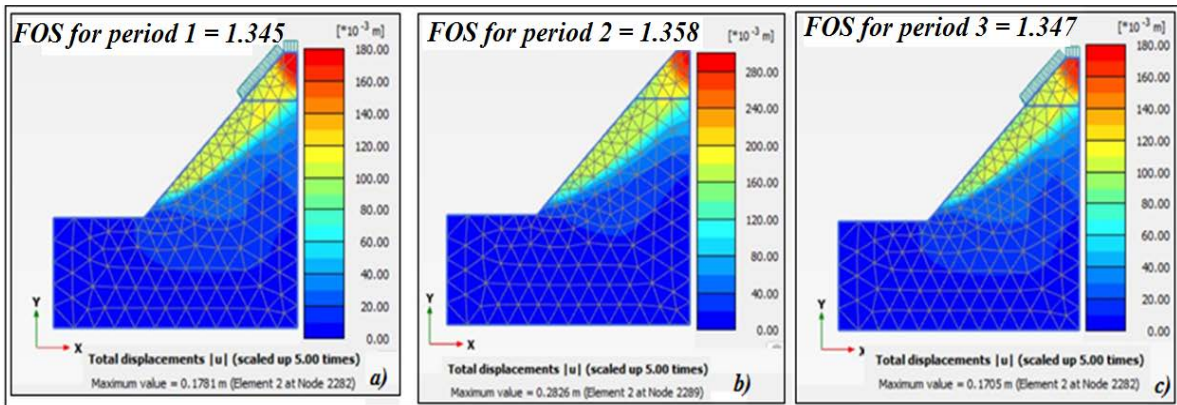


Figure 17. Case of the slope at 2.5H:1V: a) Total displacement for period 1 with the FOS value; b) Total displacement for period 2 with the FOS value; c) Total displacement for period 3 with the FOS value

Figure 16 shows the case of the embankment at 1H:1V: a) total displacement for period 2 as well as the value of the FOS, b) total displacement for period 3 as well as the value of the safety factor. Period 2 is characterized by a rainfall intensity of 0 m/d. There was no rain during this period so we considered the results before the rain and period 3 characterized by a rain intensity of 0.0048 m/d gave the following results: The stability analysis of the slope at 1H:1V during period 2 which goes from June to August gave a safety factor of around 0.7766 (Figure 16 a), a total displacement of 1.221m (Figure 16 a). The analysis of the stability of the slope at 1H:1V during period 3 from September to December gave a low safety factor of

around 0.7656 (Figure 16 b), a total displacement of 0.1693 m (Figure 16 b), the figure clearly shows that the risk of failure is present in the embankment by analyzing the color scale.

Figure 17 shows the case of the talus at 2.5H:1V, hence a) total displacement for period 1 with the FOS value, b) total displacement for period 2 with the safety factor value and c) total displacement for period 3 with the safety factor value as well. Period 1 characterized by a rain intensity of 0.0084 m/d, period 2 characterized by a rain intensity of 0 m/d as well as period 3 characterized by a rain intensity of 0.0048 m/d gave The analysis of the stability of the slope at 2.5H:1V during the first period

which goes from January to May gave a safety factor of around 1.345 (Figure 17a), a total displacement of 0.1781 m (Figure 17a). The analysis of the stability of the slope at 2.5H:1V during period 2 which goes from June to August gave a safety factor of around 1.358 (Figure 17b), a total displacement of 0.2826 m (Figure 17b). The analysis of the stability of the slope during period 3 from September to December gave a safety factor of around 1.347 (Figure 17c) and a total displacement of 0.1705 m (Figure 17c).

Table 9. presents the values of the safety factors obtained after analysis of the stability of the slopes at 1H:1V and at 2.5H:1V for periods 1, 2 and 3

Month	Monthly rainfall in mm/month	periods	Safety factor	
			Embankment at 1H:1V	Embankment at 2.5H:1V
January	412.7	Period 1	0.7625	1,345
FEBRUARY	318.6			
March	190.3			
April	262.6			
May	157			
June	0.5	Period2	0.7766	1,358
July	0			
August	0			
September	16.3	Period 3	0.7656	1,347
October	115.8			
November	176.1			
December	279.9			

Figure 18 shows the evolution of the safety factor as a function of monthly rainfall.

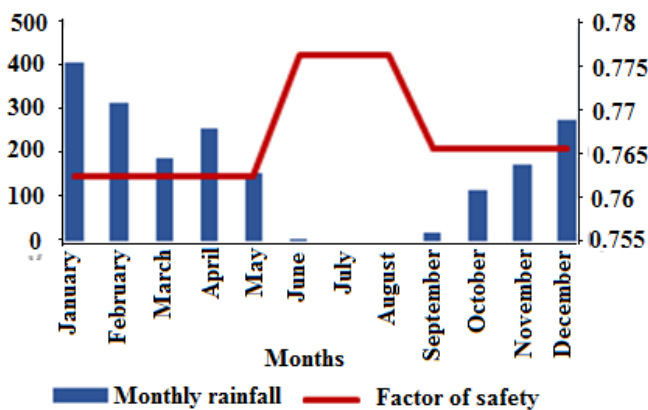


Figure18. Curve showing the evolution of the safety factor as a function of monthly rainfall [18]

5. Discussion

The stability of an embankment is analyzed by determining its safety factor. As part of our work, this analysis was carried out using the finite element method. By modeling the slope in its natural state, we obtain a safety factor of around 0.7957 with a displacement of 0.445m. this value of the safety factor shows that the natural slope is not stable because its safety factor is less than 1. Several analyzes were carried out to evaluate its stability. The 1st analysis is the influence of the slope inclination on the stability of the slope, and the results obtained during this analysis are contained in Table 6. These results show an increase in the safety factor as we

reduce the angle of the slope, that is to say that the slope which was initially unstable becomes more and more stable. We note instability in the case of the slope at 1.5H:1V and questionable stability in the cases of slopes at 2H:1V and 2.5H:1V. Thus, reducing the angle of the slope has a positive influence on the stability of the slope but in no way ensures its safety [19]. The 2nd analysis is the influence of the variation of the horizontal water table. By analyzing these results, we note that when the level of the water table is at 0 m relative to the foot of the embankment, that is to say when the water table is removed, we obtain safety factors of the order of 0.8011 and 1.3786 respectively for the slopes (1H:1V) and (2.5H:1V). At 4m from the foot of the slope (i.e. 1/H=1), the FOS are respectively 0.7653 and 1.3773 for the two slope cases. When the level of the water table is increased, the values of the FOS also increase in the two cases of slope and the values of the FS obtained at the head of the slope (that is to say at 1/H=0) are respectively of the order of 1.2841 and 1.8674 for the two cases of slope. Indeed, we note that the FOS reaches a minimum at 1/H=0.6 in the case of the slope at (2.5H:1V) then it increases further: this is due to completely slow drawdown conditions [20]. Compared to these results, we understand that submerged slope (1/H=0) is more stable than the dry slope where there is no water table as indicated by its higher FOS. Compared to these results we can say that the horizontal variation of the water table has no influence on the stability of the slope. These results are in agreement with the work of [21,20]. The 3rd analysis is the influence of vegetation on the stability of the slope. The results contained in Table 8 show that all the types of embankment studied are stable when the roots of vetiver plants have been implanted: questionable stability for the first three cases of embankment and satisfactory stability for the embankment at 2.5H: 1V with an FS>1.4. These results show that vetiver plant roots have a positive influence on the stability of the slope and support the results of [22].

The 4th analysis is the influence of infiltration on the stability of the slope. By comparing the FOS of periods 1,2 and 3 after analysis of the slopes at 1H:1V and 2.5H:1V represented in Table 9, we note that the highest FOS value compared to the others is that of the period 2; during this period, there was no rain and therefore there was also no infiltration. The safety factor of period 1 is smaller than that of period 3, this shows that there was more rain and therefore more infiltration in period 1 than in period 3. Compared to these results we can say that infiltration has a negative influence on the stability of the slope.

6. Conclusion

The city of Brazzaville has always experienced, due to its steep terrain, landslides and subsidence which raise fears of the worst. For this, it is essential to know and study the different mechanisms of landslides, their causes and the techniques and techniques for forecasting and monitoring their instabilities. The study of the stability of the natural slope using the finite element method gave a safety coefficient less than 1, indicating that the slope presents a risk of instability. To prevent this instability, a

thorough study of the embankment was carried out. The analyzes showed that rainwater infiltration affected the value of the safety factor, and we can say that they are one of the causes of the slope instabilities observed in the study area. Reducing the slope angle and establishing vetiver plant roots increased the values of the slope safety factor. The stability of this embankment therefore requires earthworks and the establishment of vegetation to guarantee its safety.

References

- [1] Khoa, D., "Modeling landslides as a bifurcation problem", *National Polytechnic Institute of Grenoble-INPG. French*. 245p. 2005.
- [2] Desodt, C., Launay, J., Molinaro, H., "Landslides, modeling and forecasting", *Ecole Normale Supérieure Paris-Saclay*. 18p. 2017.
- [3] Fourier, A., "Predicting rainfall-induced slope instability", *Proceedings of the Institution of Civil Engineers. Geotechnical Engineering*, 211 –218. 1996.
- [4] Tool, D., "Rainfall-induced landslides in Singapore", *Proceedings of the Institution of Civil Engineers: Geotechnical Engineering*, 211-216. 2001.
- [5] Rahardjo, H., Ong, T., Rezaur, R., and Leon, E., "Factors controlling instability of homogeneous soil slope under rainfall", *Journal of Geotechnical and Geoenvironment Engineering*, 1532-1543. 2007.
- [6] Kempena, A., Lacaba, R., Milan, Y., and Columbié, T., "Mapping the population due to water erosion in the city of Brazzaville", *Mineray Geology*, 144-162. 2017.
- [7] Kempena, A., Boudzoumou, F., Nganga, D., and Ray, H., "Cartography of environmental vulnerability to soil erosion of the urban area of Brazzaville using Geographic Information System (GIS)", *International Research Journal of Environment Science*, 35-43. 2014.
- [8] H. Obami-Ondon, U. Gampio Mbilou, Raymond Gentil Elenga4, Médard Ngouala Mabonzo, D. Nkounkou Tomodiatounga1, B. Mabilia, "Impact of the Seasonal Variability of the Rains on the Hydrodynamic Operation of the Aquifer Major of the Plateau of Mbe in Pool-Nord in Republic of Congo Brazzaville", *Journal of Scientific and Engineering Research*, 2019, 6(10): 173-184.
- [9] Samba, G., (2020) *The climate of Congo Brazzaville*, Paris, 2020, Edition l'harmattant, IBN 928-343-2. 244p.
- [10] Samba, K., "The climate of Lower Congo. Third cycle doctoral thesis", *University of Burgundy, CRC of Dijon*. 280p. 1978.
- [11] Denis, B., "Explanatory note for the Brazzaville-Kinkala soil map", *People's Republic of Congo. Paris: ORSTOM*. 101p. 1974.
- [12] Schwartz, D., "The soils around Brazzaville and their use", *ORSTOM, Pointe-Noire*, 45p. 1987.
- [13] Cosson, J., "Explanatory note on the Pointe-Noire and Brazzaville sheets", *Geological reconnaissance map at 1/500,000. Brazzaville: Direct. Mines and Geol. AEF*, 56p. 1955.
- [14] Dadet, P., "Explanatory note for the geological map of the Republic of Congo Brazzaville at 1:500,000, 1969 Paris: BRGM Memoirs n°70.
- [15] Boudzoumou, F., "The West Congolese chain and its foreland in the Congo: relationship with the Mayombian; sedimentation of sequences of Late Proterozoic age", *Marseille: Doctoral thesis, University of Law, Economics and Sciences of Aix-Marseille, France*. 220p. 1986.
- [16] Miyouna, T., Malounguila-Nganga, D., Essouli, O., Ndembé-Ndembé, A., Moussiéssié, J., Kinga Mouzéo., Boudzoumou, F., "Paleo-environmental study of detrital deposits of the cover formation", *CAMES-Vol 4, Num.01. ISSN 2424-7235*. 2016.
- [17] Miyouna, T., Elenga, H., Boudzoumou, F., Essouli, OF, IbaraGnianga, A., Sow, E., "Sedimentary dynamics of the Pointe Noire Cover Formation in Brazzaville, southern Republic of Congo", *Africa Science*, 15 (4), ISSN 1813-548X, 134 – 155. 2019.
- [18] Agence Nationale d'Aviation Civile (ANAC), 2023.
- [19] Pilot, G., "Landslides directly linked to works", *Revue Française de Géologie No 17, 55-69*, 1981.
- [20] Indra, N., "A contribution to the analysis of slope stability with the finite element method", *Graz University of Technology, Austria*. 133p, 2012.
- [21] Lane, PA, Griffiths, D., "Evaluation of the stability of slopes in drawdown conditions", *Journal of Geotechnical and Geoenvironmental Engineering*. Flight. 126(S), ASCE, 443-450, 2000.
- [22] Ossou, B., "Modeling the stability of an embankment using the limit equilibrium method: case of the embankment located in Ngamakosso, talangai, Brazzaville", *Master's thesis, Faculty of Science and Technology, Marien Ngouabi University, Republic of Congo*. 84p, 2022.

